18 Multiphoton Excitation and Microscopy

In the previous chapters of this book we described the emission resulting from one-photon excitation (1PE). By 1PE we mean that an excited fluorophore has reached the excited state by absorption of a single photon. We now consider two-photon (2PE) and three-photon (3PE) excitation. The term 2PE indicates that the fluorophore has reached the excited state by absorption of two photons. We will only consider simultaneous absorption of two or more photons. We will not consider sequential absorption where there is a well-defined intermediate state.

Until 1990 multiphoton spectroscopy was considered to be an exotic phenomenon that was used primarily in chemical physics and optical spectroscopy. Two-photon absorbance or excitation requires high peak powers to increase the probability that two photons are simultaneously available for absorption. Because of the interaction of two photons with the fluorophore, the selection rules for light absorption are, in principle, different from those for one-photon spectroscopy. Because of the different selection rules, two-photon spectroscopy can be used as a tool to study the excited-state symmetry of organic chromophores.[1–3] Multiphoton experiments require complex lasers and high optical powers. It did not seem possible to use multiphoton excitation (MPE) in optical microscopy because the high power would damage the biological samples. Surprisingly, MPE is now widely used in fluorescence microscopy. Multiphoton microscopy (MPM) is possible because of the favorable properties of titanium–sapphire (Ti:sapphire) lasers and the development of laser-scanning microscopes. Multiphoton excitation is usually less damaging to biological samples than in one-photon excitation. Multiphoton microscopy was introduced in 1990[4] and is now used extensively in cell imaging.[5–9]

18.1. INTRODUCTION TO MULTIPHOTON EXCITATION

The phenomenon of multiphoton excitation can be depicted in a Jablonski diagram (Figure 18.1). For one-photon absorption a single photon elevates the fluorophore to the excited state. Depending upon the absorption spectrum and the excitation wavelength the fluorophore may be excited to higher vibration levels of the S_1 state or even to the S_2 state. Irrespective of the excitation wavelength the fluorophore has reached the excited state by absorption of a single photon. Almost all fluorophores emit from the lowest energy level of the relaxed S_1 state.

MPE is accomplished using longer-wavelength excitation to avoid the much stronger single-photon absorption of the fluorophore (Figure 18.1), so that 2 or 3 photons are needed to reach the same energy level due to one-photon absorption. This diagram can give the impression that a fluorophore absorbs the photons sequentially. However, MPE is due to simultaneous absorption of multiple photons, which is why no intermediate states are shown in Figure 18.1. High illumination intensities must be used for MPE because two or more photons must interact simultaneously with the fluorophore. MPE is a nonlinear process. The extents of 2PE and 3PE are proportional to the intensity raised to the second or third power, respectively. To date all fluorophores examined with MPE have displayed the same emission spectra and lifetimes as if they were excited by one-photon absorption. Since the selection rules for optical excitation are different for 1PE, 2PE, and 3PE, the fluorophores may be placed into different excited states with different modes of excitation. However, the fluorophores emit from the same excited state, independent of one- or

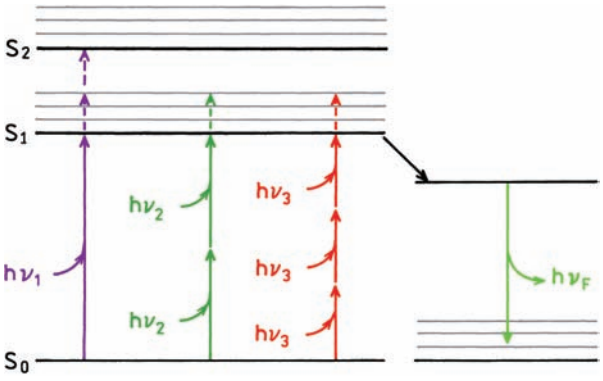

Figure 18.1. Jablonski diagram for one-, two-, and three-photon excitation.

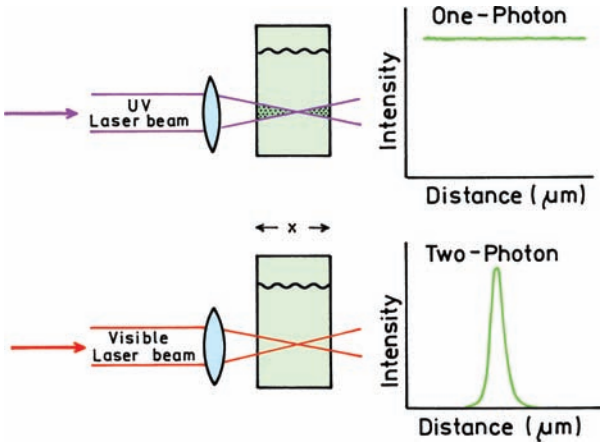

Figure 18.2. Schematic comparison of one- and two-photon excitation.

multiphoton absorption. Hence we can still use a Jablonski diagram with S_1 emission to describe multiphoton excitation.

The quadratic or higher-order dependence of MPE on the incident intensity is a favorable property for optical imaging. Assume a wavelength for 1PE is incident on a cuvette (Figure 18.2). The amount of light absorbed in any plane at a distance is proportional to the incident intensity at this plane. Focusing a beam on the center of a cuvette changes the size of the beam but does not change the total amount of light passing through a plane at a position x. The emission intensity is constant at all positions x across the cuvette, assuming the absence of inner-filter effects (top).

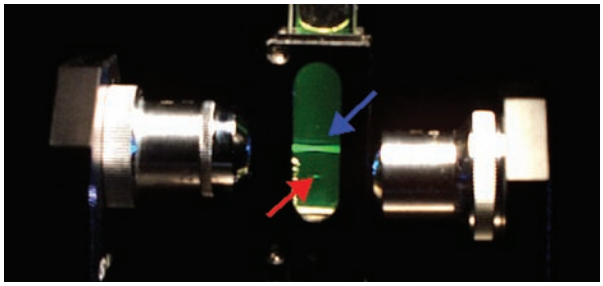

Figure 18.3. Comparison of one-photon excitation (blue arrow) and two-photon excitation (red arrow) of a fluorescein solution. Courtesy of Dr. Peter T. C. So from the Massachusetts Institute of Technology.

Now consider 2PE with a longer wavelength. The amount of light absorbed is proportional to the square of the intensity. Focusing the beam decreases its size but increases its intensity. As a result the amount of light absorbed is not constant across the cuvette, but shows a maximum at the focal point where the incident intensity is highest (Figure 18.2, bottom). This effect can result in strongly localized excitation. Figure 18.3 shows a fluorescein solution illuminated with wavelengths for 1PE and 2PE. For 1PE the fluorescein is excited across the cuvette. For 2PE the fluorescein is only excited in a small spot at the focal point of the laser beam.

Most fluorophores photobleach rapidly in fluorescence microscopy. Localized excitation is an advantage under these conditions. If a biological sample undergoes 1PE the light is absorbed at all depths in the sample, not just in the focal plane.[11–12] As a result the entire thickness of the sample undergoes photobleaching (Figure 18.4, left) and photodamage occurs across the entire thickness of the sample.

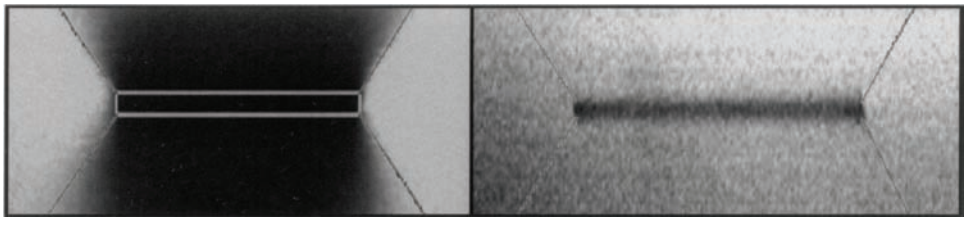

Figure 18.4. Photobleaching of rhodamine in a Formvar layer with one- (left) and two-photon excitation (right). From [12].

For three-dimensional reconstruction of the cell image it is necessary to obtain images from multiple focal planes. This is difficult with 1PE because all planes are bleached irrespective of the position of the focal plane.

The right side of Figure 18.4 shows photobleaching with 2PE, which is now strongly localized in the focal plane. The fluorophores are still photobleached, but it is possible to image above and below the focal plane because the fluorophores in these regions are not photobleached. The adverse effects due to absorption are localized to the focal plane, which may be less damaging to the specimen than when photobleaching occurs across the entire thickness. MPE is usually performed using wavelengths from 720 to 950 nm, where there is minimal absorption by water and intrinsic chromophores (see Figure 19.4).

18.2. CROSS-SECTIONS FOR MULTIPHOTON ABSORPTION

We are all familiar with the absorption coefficients for one-photon absorption, which are usually expressed as the molar extinction coefficients in units of M^{-1} cm^{-1}. For a single molecule the absorption can be described in units of cm^2, which is the effective area over which a single molecule absorbs the incident light. For 1PE the optical cross-sections σ_1 range from 10^{-15} to 10^{-17} cm^2. Cross-sections of 10^{-15}, 10^{-16}, and 10^{-17} cm^2 correspond to squares with sides of 3, 1, and 0.3 Å, respectively. One-photon cross-sections are thus comparable to the size of fluorophores and can be understood intuitively.

It is more difficult to have an instructive understanding of cross-sections for multiphoton absorption. For 2PE the cross-sections are in units of cm^4 s/photon. The values of the 2PE cross-sections are reported in terms of GM (Goppert-Mayer) units, where 1 GM = 10^{-50} cm^4 s/photon. The units are named after Maria Goppert-Mayer, who developed the theory for two-photon absorption processes.[13–14] These units for the 2PE cross-sections are more difficult to understand than the cross-sections for 1PE in units of area.

The physical origin of the 2PE cross-sections can be understood by some simple considerations. For one-photon absorption the number of photons absorbed per second (NA_1) is given by

$$NA_1\ (\text{photon/s}) = \sigma_1\ (\text{cm}^2)\ I(\text{photon/cm}^2\text{s}) \qquad (18.1)$$

where I is the intensity and σ_1 is the cross-section for one-photon absorption. The units are given within the parentheses. The cross-section in cm^2 is multiplied by the number of photons passing near the molecule per second to yield the number of photons absorbed per second. To obtain NA_1 in photons per second the cross-section must be in units of cm^2.

Now consider two-photon absorption. The number of photons absorbed per second by 2PE (NA_2) is given by

$$NA_2\ (\text{photons/s}) = \sigma_2 I^2(\text{photons/cm}^2\text{s})^2 \qquad (18.2)$$

In order for the units to match on both sides of eq. 18.2 the units of σ_2 must be cm^4s/photon. Similarly, for 3PE,

$$NA_3\ (\text{photons/s}) = \sigma_3 I^3(\text{photons/cm}^2\text{s})^3 \qquad (18.3)$$

and the units of a three-photon cross-section are cm^6 s^2/photon^2.

18.3. TWO-PHOTON ABSORPTION SPECTRA

Since selection rules for one- and two-photon optical transitions are different there is no reason to expect the one- and two-photon absorption spectra to be the same.[15–17] Figure 18.5 shows these spectra for some commonly used fluorophores. Note that the *y*-axis is a logarithmic scale and the one-photon spectra are plotted on an arbitrary scale. For visual comparison the spectra are usually plotted on the same wavelength scale where the one-photon spectrum is plotted using twofold longer wavelengths. The *x*-axis is usually the wavelengths used for two-photon absorption measurements. Occasionally the data are plotted on the one-photon wavelength scale. The correct scale is usually apparent from the known one-photon absorption spectra of the fluorophores.

The one- and two-photon absorption spectra are different for the three fluorophores shown in Figure 18.5, which has been found for most fluorophores.[15–17] An important feature of the two-photon absorption is that, on a relative scale, the absorption is stronger at wavelengths below twice the long-wavelength absorption. For example, the one-photon absorption of RhB is much weaker at 400 nm than at 500 nm (middle panel). The two-photon absorption is stronger for RhB at 800 nm than at 1000 nm. This is convenient because two-photon microscopy is almost exclusively done using Ti:sapphire lasers, which have an output from 720 to 1000 nm. Additionally, the shape of the two-photon absorption spectra often allows simultaneous excitation of several fluorophores using a single wavelength.

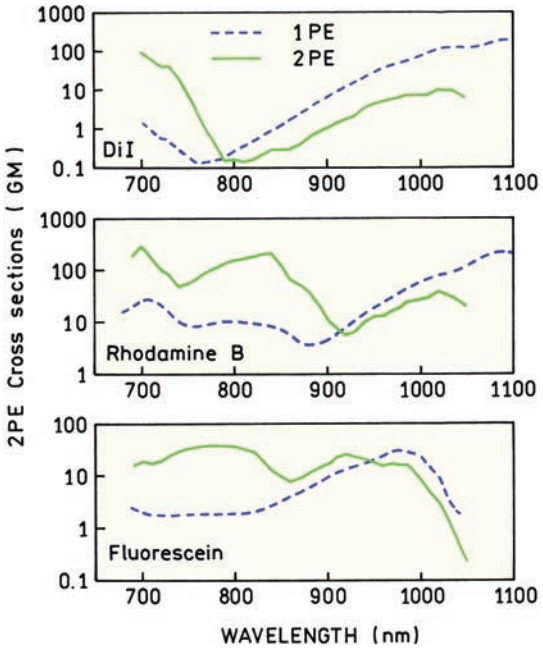

Figure 18.5. One- and two-photon absorption spectra of three commonly used fluorophores. The one-photon spectra are plotted on an arbitrary scale. From [17].

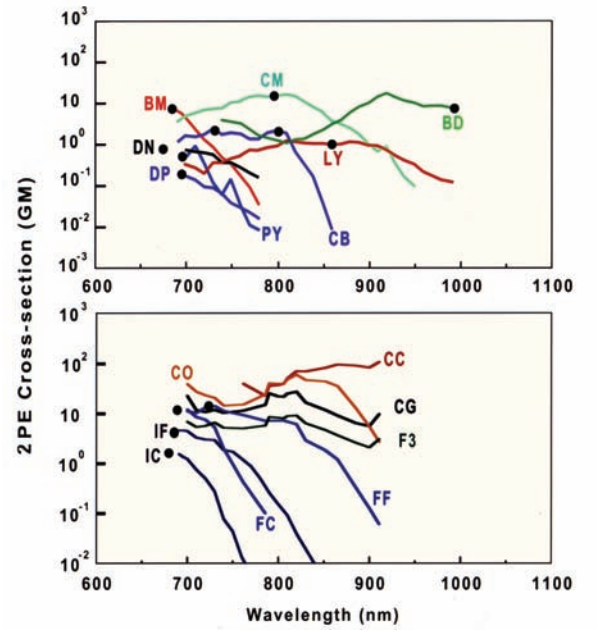

Figure 18.6. Two-photon fluorescence excitation spectra of fluorophores. For BM (Bis-MSB), data represent two-photon absorption cross-sections. For all the other fluorophores, data represent two-photon action cross-sections—i.e., the product of the fluorescence emission quantum efficiencies and the two-photon absorption cross-sections. Units are Goppert-Mayer (GM); 1 GM = 10^{-50} cm^4 s/photon. Spectra are excited with linearly polarized light using a mode-locked Ti:sapphire laser. The black dot indicates twice the wavelength of the one-photon absorption maximum of the fluorophore. The fluorophores illustrated in *a* are as follows: BM, *p*-bis(*o*-methylstyryl)-benzene; CB, Cascade Blue hydrazine trisodium salt; LY, Lucifer Yellow CH ammonium salt; BD (BODIPY), 4,4-difluoro-1,3,5,7,8-pentamethyl-4-bora-3*a*,4*a*-diazaindacene-2,6-disulfonic acid disodium salt; DP (DAPI not DNA bound), 4',6-diamidino-2-phenylindole dyhydrochloride; DN (dansyl), 5-dimethylaminonaphthalene-1-sulfonyl hydrazine; PY, 1,2-bis-(1-pyrenedecanoyl)-*sn*-glycero-3-phosphocholine; and CM, coumarin 307. The fluorophores illustrated in *b* are as follows: IC, indo-1 with Ca^{2+}; IF, indo-1 without Ca^{2+}; FC, fura-2 with Ca^{2+}; FF, fura-2 without Ca^{2+}; CG, calcium green-1 with Ca^{2+}; CO, calcium orange with Ca^{2+}; CC, calcium crimson Ca^{2+}; and F3, fluo-3 with Ca^{2+}. From [17].

Additional two-photon absorption spectra are shown in Figure 18.6. It is difficult to measure their spectra because the amount of light absorbed depends strongly on the exact spatial and temporal profile of the pulses.[18–19] For this reason two-photon cross-sections are usually measured relative to a standard, typically bis-MSB, which appears to be the best characterized two-photon standard.[20] Fortunately, fluoresceins have large cross-sections at Ti:sapphire wavelengths. The cross-sections of UV-absorbing fluorophores such as indo-1 (IC) or fura-2 with calcium (FC) are small—above 700 nm—because two photons at wavelengths above about 700 nm do not contain enough energy to reach the S_1 state.

One-photon absorption spectra often show regions of low absorption at wavelengths below the long-wavelength absorption. For instance, see the absorption spectra of fluorescein (Figure 3.9) or dyes used for DNA sequencing. The low absorption at wavelengths below the $S_0 \otimes S_1$ transition makes it difficult to excite more than one dye at a time using a laser source. The larger width of the two-photon absorption spectra makes it easier to excite multiple fluorophores using one wavelength. This possibility is shown in Figure 18.7 for five fluorophores that were all excited using 800 nm from a Ti:sapphire laser.

18.4. TWO-PHOTON EXCITATION OF A DNA-BOUND FLUOROPHORE

At present MPE is used primarily for cellular imaging or for fluorescence correlation spectroscopy (Chapter 24). Both of these applications make use of the small excited volumes obtained using MPE with a focused laser beam. Prior to describing MPE microscopy it is informative to see the effects of MPE on the fluorophores themselves.[22] Figure 18.8 shows emission spectra of DAPI bound to DNA when

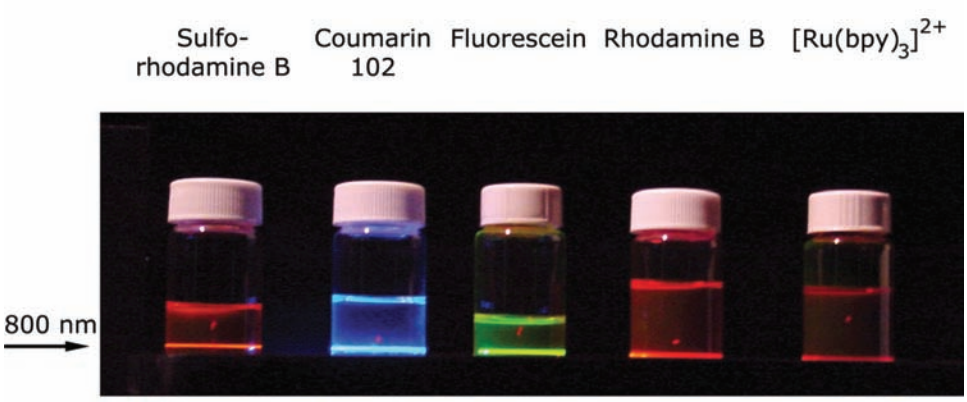

Figure 18.7. Simultaneous excitation of several fluorophores using the 800-nm output of a regeneratively amplified Ti:sapphire laser. The laser is incident near the bottom of the bottles. The upper lines are reflections off the surface. From [21].

excited at 360, 830, and 885 nm.[23–25] The emission spectra are the same at each excitation wavelength, showing that emission occurs from the lowest singlet state irrespective of the mode of excitation (Section 18.1). Although not shown, the intensity decays are the same for these excitation wavelengths.[24] When excited at 360 nm a twofold decrease in the incident intensity results in a twofold decrease in fluorescence intensity, as expected for a one-photon process. When excited at 830 and 885 nm, the emission intensity decreases four- and eight-fold, respectively. This indicates that 2PE occurs at 830 nm and 3PE occurs at 885 nm.

The mode of excitation can be determined by the dependence of the emission intensity on incident power (Figure 18.9). For excitation at 830 and 885 nm a plot of DAPI emission intensity versus incident power yields slopes of 2.01 and 2.85, respectively. The mode of excitation switches from 2PE to 3PE between these wavelengths. The reason for this switch can be found in the DAPI absorption spectrum (top). The long-wavelength absorption ends near 420 nm. Above 840 nm 2PE can no longer occur because the energy of the combined photons is not adequate

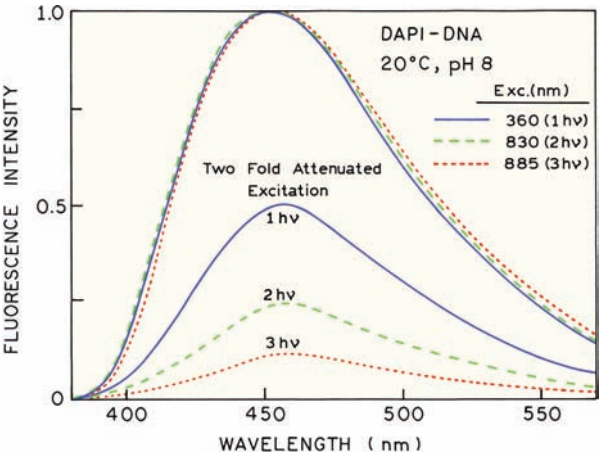

Figure 18.8. Normalized emission spectra of DAPI-DNA for excitation at 360, 830, and 885 nm. Also shown are the emission spectra with a twofold attenuation of the excitation. The excitation source at 830 and 885 nm was a femtosecond Ti:sapphire laser; 80 MHz repetition rate with a pulse width near 80 fs.

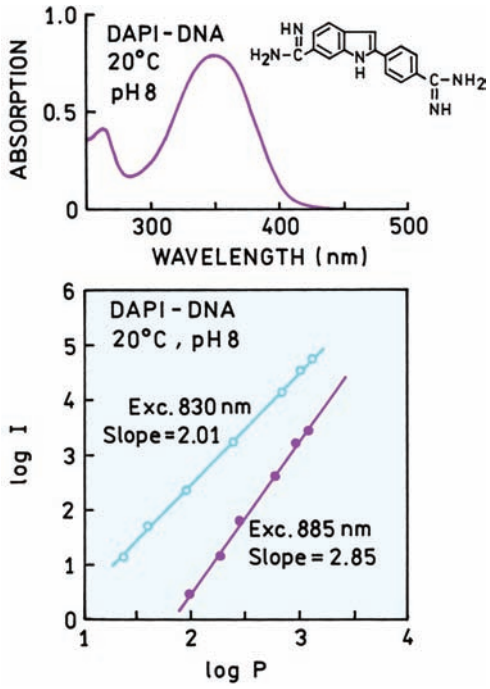

Figure 18.9. Absorption spectra and power-dependent intensities of DAPI-DNA. The laser power is in milliwatts. From [24].

to reach the S_1 state. As a result the mode of excitation changes to 3PE. The 2PE-to-3PE transition occurs on the long-wavelength edge of the DAPI absorption. This is a result of the 2PE cross-section being much larger than the 3PE cross-section, so that 2PE dominates wherever possible. It was initially surprising that 3PE could be observed without detectible damage to the sample.

18.5. ANISOTROPIES WITH MULTIPHOTON EXCITATION

In the previous section we saw that the emission spectra of DAPI are the same for one, two, and three-photon excitations. In contrast, the anisotropies can be very different for each mode of excitation.[26–32] There are two reasons for the different anisotropies. Fundamental anisotropies can be different for each mode of excitation. This is a complex topic that we will not describe. The second reason is because excitation photocorrelation is different depending on the mode of excitation. More specifically, two-photon excitation results in a more strongly aligned population because this process depends on $\cos^4\theta$ photoselection, rather than $\cos^2\theta$ for one-photon excitation.

To avoid confusion we note that there are two types of polarization experiments in multiphoton spectroscopy. The experiments described in this book use only linearly polarized light, and the emission anisotropy value is determined by the motions of fluorophores in the excited state. A different type of polarization experiment is performed in chemical physics. These experiments compare the absorption of linearly and circularly polarized light, which provides information about the symmetry of the excited states.[33–35]

18.5.1. Excitation Photoselection for Two-Photon Excitation

In section 10.2 we showed that an anisotropy is related to the average value of $\cos^2\theta$. The fundamental anisotropy value of 0.4 for one-photon excitation is a consequence of $\cos^2\theta$ photoselection. For two-photon excitation the fluorophore interacts simultaneously with two photons, and each interaction is proportional to $\cos^2\theta$. Hence, the photoselection function becomes[29]

$$f_2(\theta) = \cos^4\theta \sin\theta \, d\theta \qquad (18.4)$$

Introduction of this function into the calculation of $\langle\cos^2\theta\rangle$ (eq. 10.21) allows calculation of the anisotropies expected for collinear transitions (Table 10.1). For $\beta = 0$ the fundamental anisotropy for two-photon excitation is 0.57, rather than 0.4. For three-photon excitation the fundamental anisotropy can be as large as 0.66 (Figure 18.10 and Table 18.1).

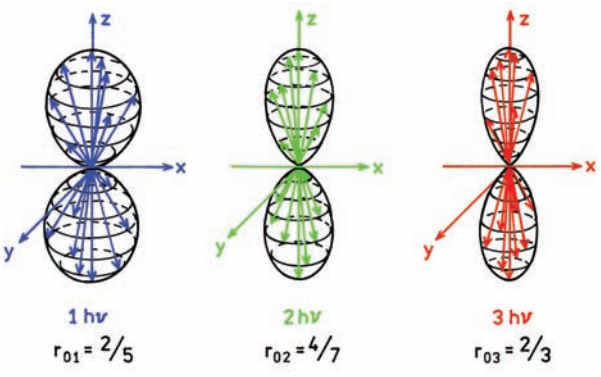

Figure 18.10. Excited-state distributions for $r_0 = 0.40$ with one-, two-, and three-photon excitation.

It is important to recognize the meaning of these anisotropy values. A value of 0.4 for one-photon excitation and a value of 0.57 for two-photon excitation both mean the absorption and emission transition moments are parallel. There is no new information in the higher anisotropy value for two-photon excitation, except for confirming the transition moments are still parallel. In some cases the anisotropies do not follow the predictions based on $\cos^2\theta$ or $\cos^4\theta$ photoselection. One example is tryptophan and indole, which display lower anisotropies with two-photon excitation (Section 18.7).

18.5.2. Two-Photon Anisotropy of DPH

It is instructive to see how the anisotropy depends on the mode of excitation. Figure 18.11 shows the excitation anisotropy spectra of DPH. For one-photon excitation (340–380 nm), the anisotropy in frozen solution is always

Table 18.1. Fundamental Anisotropies for One-, Two-, and Three-Photon Excitation[a]

β (deg)	One-photon r_{01}	Two-photon r_{02}	Three-photon r_{03}
0	0.40	0.57	0.66
45	0.10	0.41	0.17
54.7	0.00	0.00	0.00
90	–0.20	–0.29	–0.33

[a]Data from [35].

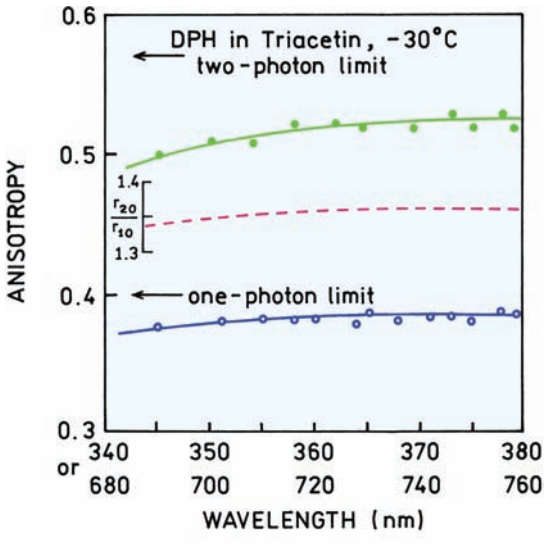

Figure 18.11. Excitation anisotropy spectra of DPH in frozen solution for one- and two-photon excitation. Revised with permission from [36]. Copyright © 1994, American Institute of Physics.

below the one-photon limit of 0.40. For two-photon excitation the anisotropy is near 0.5, well above the one-photon limit. The larger anisotropy for two-photon excitation is mostly due to $\cos^4\theta$ photoselection. This can be seen from the ratio of the one- and two-photon anisotropies. This ratio is near 1.35, which is close to the predicted ratio of 1.425 (Table 18.1). These data indicate that the value of β for DPH is nearly the same for one- and two-photon excitation. Anisotropy values larger than 0.57 have been observed with three-photon excitation.[32]

18.6. MPE FOR A MEMBRANE-BOUND FLUOROPHORE

Multiphoton excitation requires high local light intensities, which is obtained from focused laser beams. Hence, it is natural to ask whether these conditions are compatible with studies of biological molecules. Remarkably, multiphoton excitation is possible without significant heating or damage of many samples. Figure 18.12 shows emission spectra of DPH in DPPG vesicles, and Figure 18.13 shows the intensity decays for the same sample.[36–38] The same emission spectra and nearly the same intensity decay were observed with 1PE and 2PE, suggesting the membrane is not damaged by the locally intense excitation. The anisotropy decay of DPH is more sensitive to the temperature of the membrane than the intensity decay. The anisotropy decay of DPH in DPPG was essentially the same for 1PE and 2PE,

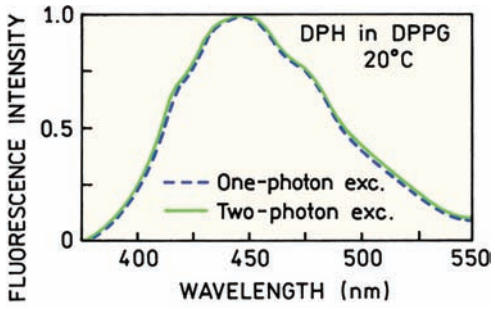

Figure 18.12. Fluorescence emission spectra of DPH in DPPG bilayers for excitation at 358 nm (dashed) and 716 nm (solid). From [36].

except for the photoselection factor (Figure 18.14). This result indicates that the membrane is not heated during 2PE of DPH. Remarkably, even three-photon excitation did not seem to elevate the temperature of the membranes (Figure 18.15). The steady-state anisotropies with 1PE and 3PE show phase transitions at the same temperature. The minimal effect of MPE on biomolecules has been demonstrated by continued viability of hamster embryos even after extensive multiphoton imaging.[39]

18.7. MPE OF INTRINSIC PROTEIN FLUORESCENCE

Fluorescence microscopy is rarely performed using intrinsic protein fluorescence because of the difficulty in trans-

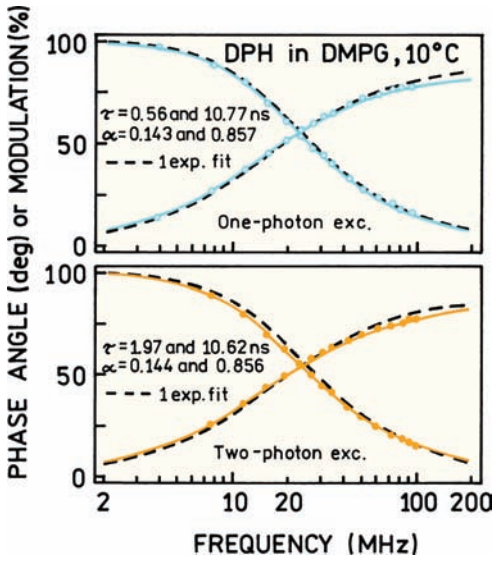

Figure 18.13. Frequency-domain intensity decay for DPH in DMPG vesicles, 10°C, for one-photon excitation at 358 nm (top) and two-photon excitation at 716 nm (bottom). From [36].

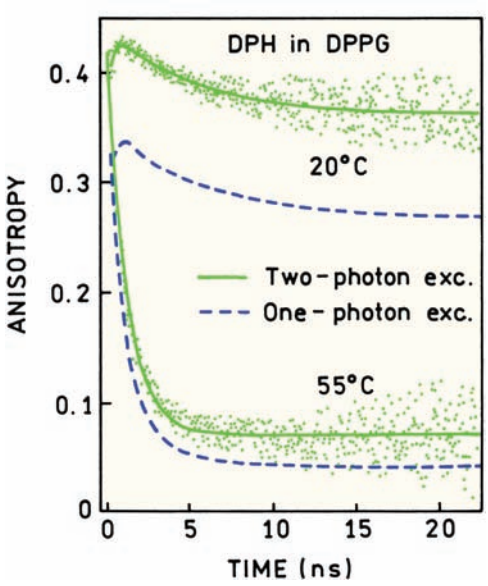

Figure 18.14. Time-domain anisotropy decay of DPH in DPPG bilayers for one- and two-photon excitation. From [37].

mitting UV light through the optical components. This problem can be avoided using two-photon excitation because the required wavelength near 560–600 nm is easily transmitted. Several reports have appeared on 2PE of proteins in solution.[40–45] Ti:sapphire lasers do not provide output at the wavelengths needed for 2PE of proteins, and Ti:sapphire lasers are presently the optimal choice for multiphoton microscopy.

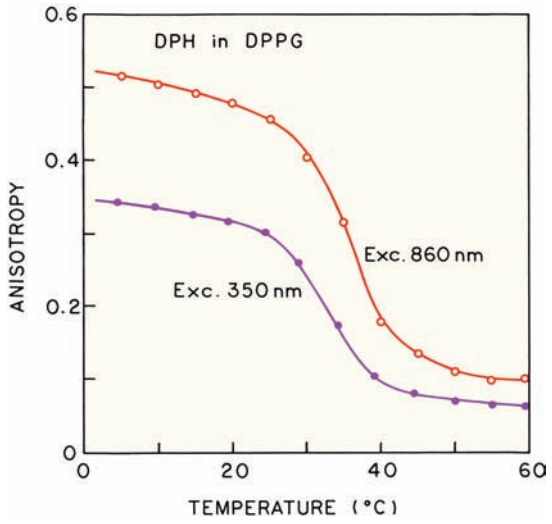

Figure 18.15. Temperature-dependent anisotropies of DPH in DPPG for three-photon excitation at 860 nm and one-photon excitation at 350 nm. From [38].

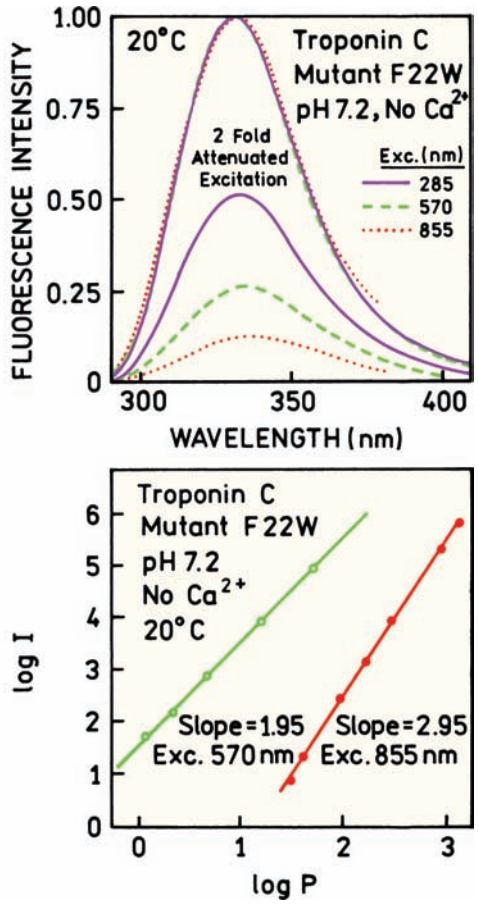

Figure 18.16. Emission spectra of troponin C F22W with one-, two-, and three-photon excitation. 570 nm was obtained from a cavity-dumped dye laser. The lower panel shows the dependence of the emission intensity on incident power, in mW. From [47].

The problem of exciting tyrosine and tryptophan fluorescence with a Ti:sapphire laser was solved by using three-photon excitation. Wavelengths near 850 nm can be used for three-photon excitation of tryptophan.[46–47] Multiphoton excitation of proteins is illustrated in Figure 18.16 for a mutant of troponin C (TnC). This protein from muscle typically contains only tyrosine residues. The TnC mutant contains a single tryptophan residue replacing a phenylalanine residue at position 22 (F22W). Emission spectra are shown for excitation at 285 nm, and at the unusual wavelengths of 570 and 855 nm. The same emission spectra were observed for all three excitation wavelengths. Since 570 and 855 nm are much longer than the last absorption band of tryptophan, the emission observed with these excitation wavelengths cannot be due to the unusual process of one-photon excitation.

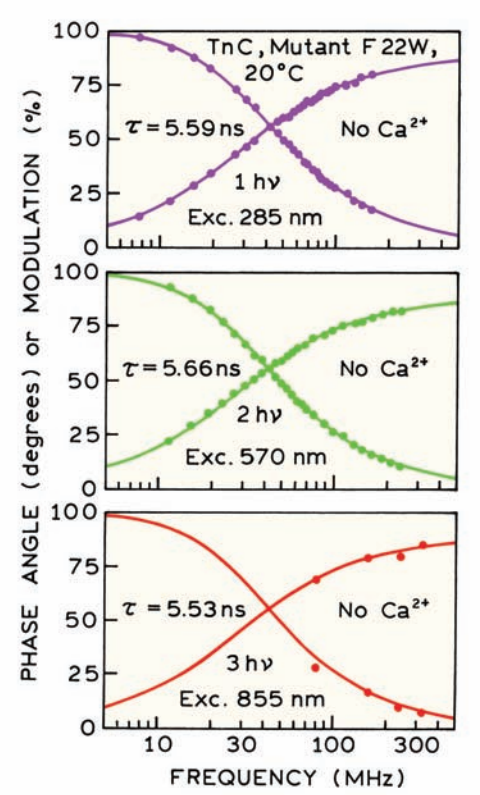

Figure 18.17. Frequency-domain intensity decays of TnC F22W without Ca^{2+} for one-, two-, and three-photon excitation. From [47].

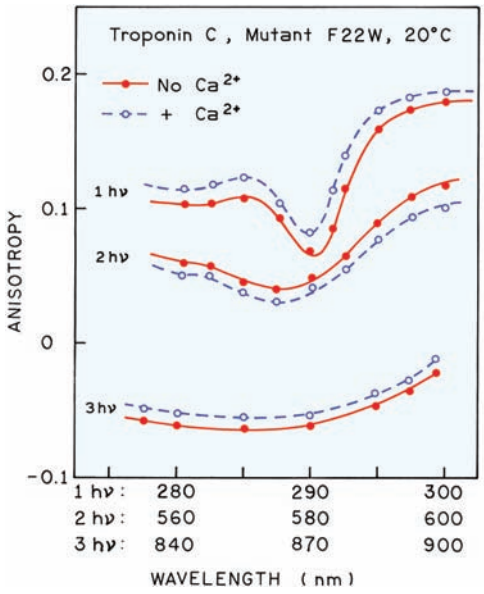

Figure 18.18. Excitation anisotropy spectrum of TnC mutant F22W for one-, two-, and three-photon excitation. From [47].

The nature of the excitation process is revealed by the effects of attenuating the intensity of the incident light. At 285 nm a twofold decrease in the incident light results in a twofold decrease in the emission intensity, which is the usual result for one-photon excitation where the intensity of the emitted light is directly proportional to the excitation intensity. For excitation at 570 nm, twofold attenuation of the incident light results in a fourfold decrease in emission intensity. At 855 nm the same twofold decrease in incident intensity results in an eight-fold decrease in emission intensity. The emission intensity depends on the square of the incident intensity at 570 nm, and on the cube of the incident intensity at 855 nm (Figure 18.16). This data indicates that the emission with 570-nm excitation is due to two-photon excitation, and the emission with 855-nm excitation is due to three-photon excitation. The tryptophan intensity decay is the same for each excitation wavelength (Figure 18.17), which suggests the protein was not adversely affected by the intense 855 nm excitation.

Another feature for multiphoton excitation is the opportunity for new spectroscopic information. This is illustrated by the unusual anisotropies displayed by tryptophan with two- or three-photon excitation. Surprisingly, the anisotropies of the tryptophan residue in TnC F22W are lower for two-photon excitation (560–600 nm) than for one-photon excitation (280–300 nm, Figure 18.18). The anisotropies are still lower for three-photon excitation (840–900 nm). Multiphoton excitation is expected to result in higher anisotropies due to $\cos^4\theta$ or $\cos^6\theta$ photoselection. The lower anisotropies for tryptophan observed for MPE suggest that MPE is occurring primarily to the ^1L_b state of tryptophan, with emission as usual from the ^1L_a state. Apparently, MPE to the ^1L_b state displays a higher MPE cross-section than does the ^1L_a state, but a full explanation may require more complex analysis.[48–49]

It is of interest to understand how multiphoton excitation is accomplished. The 570-nm excitation was obtained from the cavity-dumped pulses from a rhodamine 6G dye laser. These pulses are about 7 ps wide. Excitation at 855 nm was accomplished using pulses from a Ti:sapphire laser, which are about 70 fs wide. Pulsed excitation is used because it is necessary to have a high instantaneous density of photons in order to have a significant probability of MPE.

At present we are not aware of 3PE of intrinsic protein fluorescence using optical microscopy. However, 3PE of serotonin (5-hydroxytryptamine) has been used in microscopy to image granules of this neurotransmitter in

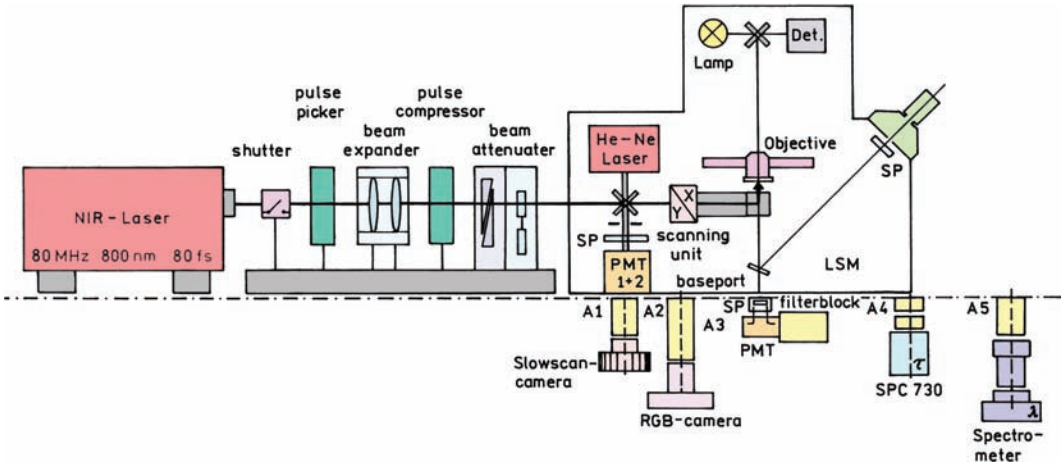

Figure 18.19. Schematic of a multiphoton microscope. Revised from [52].

intact cells,[50] but serotonin may undergo complex photochemistry with MPE.[51]

18.8. MULTIPHOTON MICROSCOPY

At present the dominant use of MPE is for optical imaging. Multiphoton microscopy (MPM) requires complex instruments that are often maintained by dedicated personnel. Most MPMs use a Ti:sapphire laser source (Figure 18.19). There may be a pulse picker to decrease the repetition rate. The optical path contains components for focusing the beam and for adjusting its intensity. In order to obtain an image the focused laser beam is raster scanned across the sample by the scanning unit. In this instrument there is also a CW He–Ne laser for conventional confocal laser-scanning microscopy (CLSM) with one-photon excitation. When using MPE all the emitted light comes from the focal spot, and there is minimal out-of-plane fluorescence. For this reason the multiphoton-induced fluorescence is usually measured using a PMT behind the objective, which provides higher sensitivity than passing the emission back through the scanning unit as is done with CLSM.

Several detectors are shown below the baseplate of the microscope. Prior to reaching the detector the signal is passed through a short-pass (SP) filter to remove the longer-wavelength excitation from the emission. Separate detectors are available for measuring lifetimes or emission spectra.

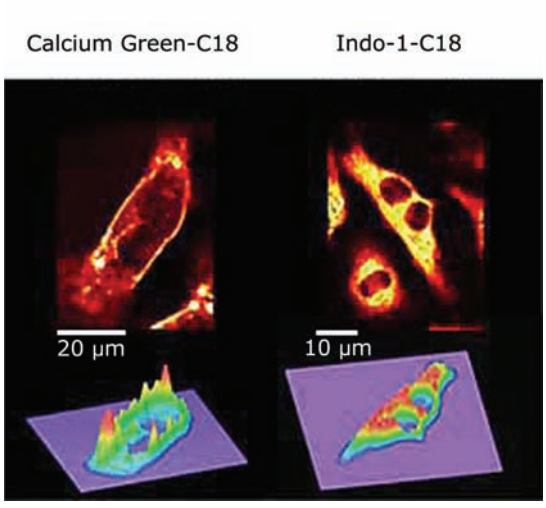

Figure 18.20. Multiphoton microscopy images of neonatal rat cells labeled with lipid conjugate of Calcium Green (CG-C18) or Indo-1 (Indo-1-C18). From [54].

18.8.1. Calcium Imaging

Multiphoton microscopes have been used extensively for cellular imaging. We present just a few examples. MPM can be used for calcium imaging. Figure 18.20 shows neonatal rat cells labeled with a lipid conjugate of Calcium Green (left) or the lipid conjugate Indo-1 (right).[53–54] The two probes show different intracellular distributions. The different distributions occur because CG-C18 localizes on the outside of the cell and Indo-1-C18 was internalized and distributed throughout the cell except for the nucleus.

Multiphoton excitation microscopy is used to measure rapid signaling events in cells.[55] HeLa cells were transfected with the cDNA for a cameleon calcium sensor (Figure

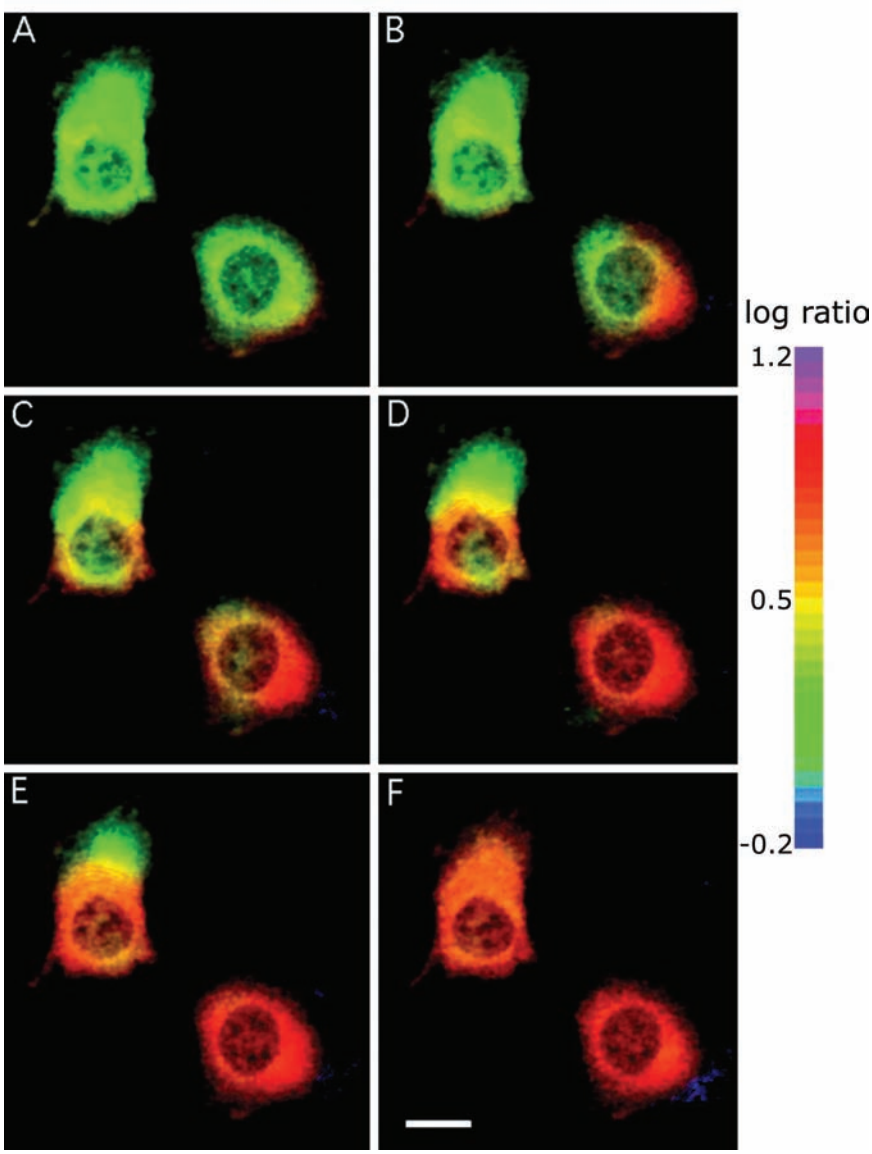

Figure 18.21. Fluorescence intensity ratios from a cameleon calcium sensor for HeLa cells locally exposed to histamine. The images were recorded at 1 second intervals starting 1 second before exposure to histamine. The intensity ratio is 535 nm/480 nm. Scale bar is 10 μm. Reprinted with permission from [55].

18.21). These sensors are composed of a donor–acceptor GFP pair connected by a calcium-sensitive linker.[56] The linker consists of calmodulin and the M13 peptide. In the presence of calcium the peptide binds to calmodulin, bringing the donor and acceptor closer together and increasing the extent of energy transfer. The first image was taken 1 second before local exposure to histamine. Exposure to histamine results in a calcium wave that travels across the cell in about 4 seconds.

18.8.2. Imaging of NAD(P)H and FAD

The intracellular concentrations of NAD(P)H and FAD reflect the energy metabolism of cells. Figure 18.22 shows fluorescence images of an isolated cardiac myocyte with excitation at 750 nm.[57] The images were recorded in two wavelength regions. The image is brighter at shorter wavelengths, where the NADH emission is expected to be dominant, and weaker at wavelengths where FAD emits. There can be numerous reasons for the difference in intensity in

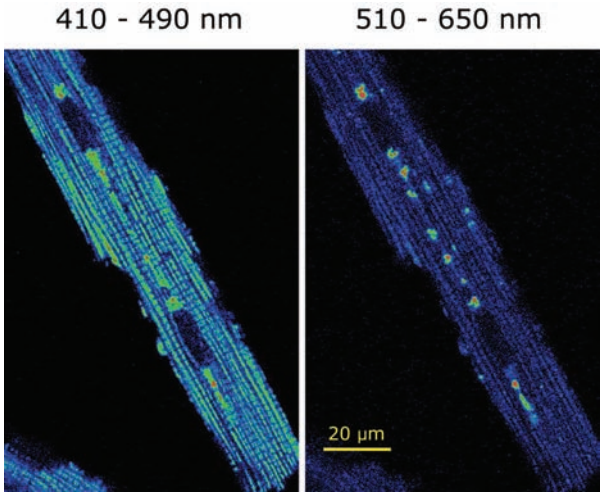

Figure 18.22. Two-photon induced fluorescence images of a cardiac myocyte observed at 410–490 nm (left) and 510–650 nm (right). Excitation at 750 nm. From [57].

these wavelength regions, such as the concentrations and quantum yields of these cofactors in the cells. Part of the explanation lies in the two-photon cross-sections of NADH and FAD (Figure 18.23). At 750 nm the cross-section of NADH is smaller than that of FAD. If a longer excitation wavelength were used the FAD emission may dominate the emission.

18.8.3. Excitation of Multiple Fluorophores

In Section 18.2 we described the two-photon absorption spectra of fluorophores. These spectra indicated that multiple fluorophores could be excited by MPE at a single wavelength. This possibility is demonstrated in Figure 18.24 for RBL cells labeled with four different fluorophores, each specific for a different region of the cell. All four fluorophores could be excited using a single wavelength. Given the one-photon absorption spectra of these probes, and the autofluorescence with UV excitation, it is very unlikely that such images could be obtained using one-photon excitation.

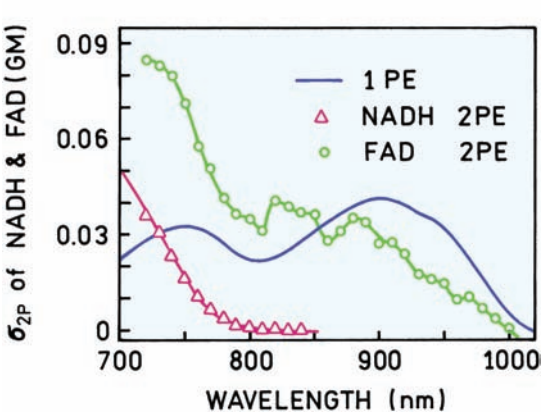

Figure 18.23. One-photon absorption spectra of FAD (——) and NADH (—Δ—). Also shown are the two-photon cross-sections for FAD (○) and NADH (Δ). Revised from [57].

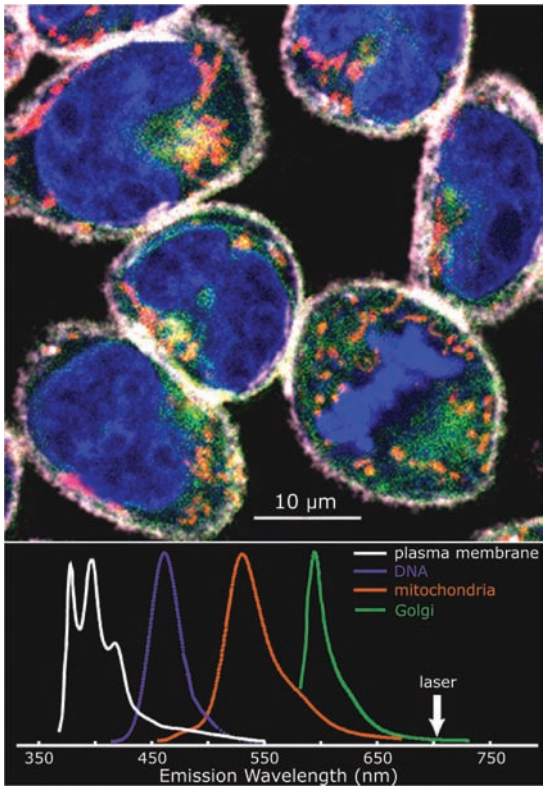

Figure 18.24. Multiphoton excitation images of rat basophilic leukemia (RBL) cells labeled with four probes: a plasma membrane label (pyrene lysophosphatidylcholine), a nuclear strain (DAPI), a Golgi label (Bodipy sphingomyelin), and a mitochondrial stain (rhodamine 123). From [17] and courtesy of Dr. Watt Webb from Cornell University, N.Y.

18.8.4. Three-Dimensional Imaging of Cells

A longstanding goal of multiphoton microscopy has been to obtain three-dimensional cellular images.[58–59] This is possible because the localized excitation allows collection of images at various focal planes in the cell (Figure 18.25, left). Using these 2D images it is possible to reconstruct a 3D image. Figure 18.26 shows a 3D reconstruction of a live PC12 cell stained with acridine orange. This probe emits in the green when bound to nuclear DNA and red when present in acidic organelles.

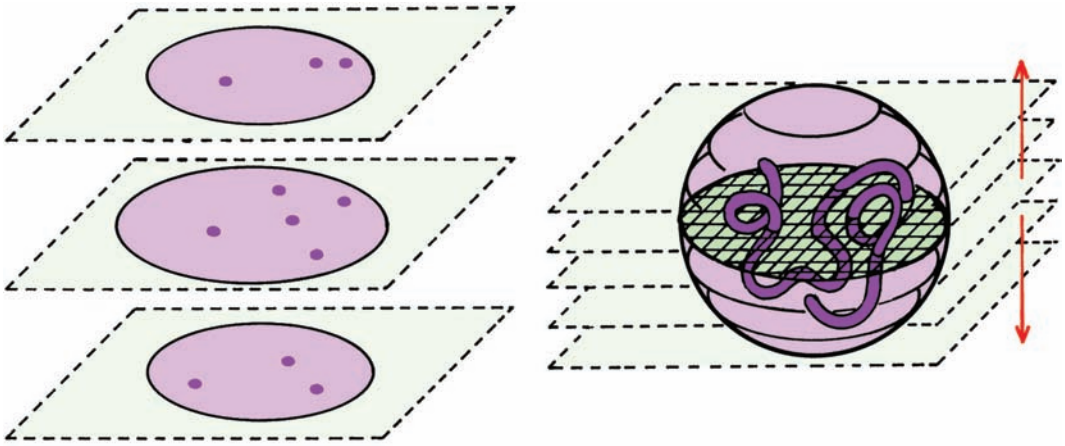

Figure 18.25. Three-dimensional cell imaging using confocal or multiphoton microscopy.

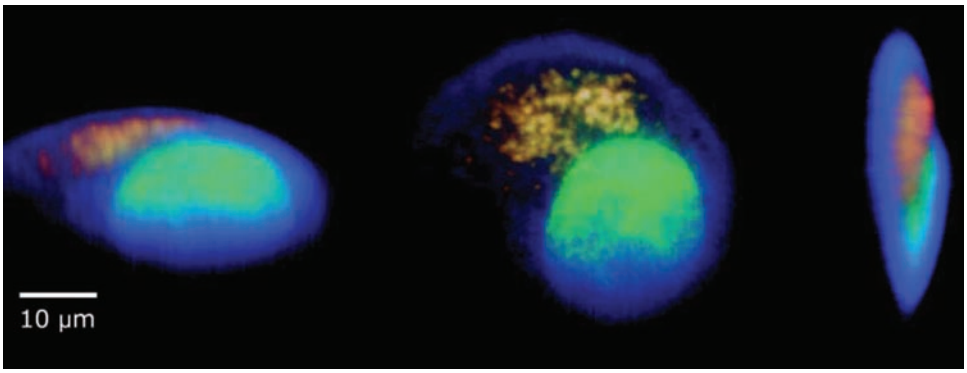

Figure 18.26. Three-dimensional reconstruction of a live PC cell stained with acridine orange, which emits green (525 nm) when bound to DNA and red (650 nm) when present in acidic organelles. The perspective on the left is rotated 60° from the cells around the horizontal axis. The perspective on the right is rotated 90° around the vertical axis. Figure courtesy of Dr. Stefan Hall, Max-Planck Institute for Physical Chemistry, Göttingen, Germany.

REFERENCES

1. Friedrich DM, McClain WM. 1980. Two-photon molecular electronic spectroscopy. *Annu Rev Phys Chem* **31**:559–577.
2. Wirth MJ, Koskelo A, Sanders MJ. 1981. Molecular symmetry and two-photon spectroscopy. *Appl Spectrosc* **35**:14–21.
3. Birge RR. 1983. One- and two-photon excitation spectroscopy. In *Ultrasensitive laser spectroscopy*, pp. 109–174. Ed DS Kliger. Academic Press, New York.
4. Denk W, Strickler JH, Webb WW. 1990. Two-photon laser scanning fluorescence microscopy. *Science* **248**:73–76.
5. Masters BR, ed. 2003. *Selected papers on multiphoton excitation microscopy*. *SPIE milestone series*, SPIE Optical Engineering Press, Bellingham, WA.
6. Diaspro A, ed. 2002. *Confocal and two-photon microscopy foundations, applications, and advances*. Wiley-Liss, New York, 56.
7. Hell SW, ed. 1996. *Bioimaging special issue on nonlinear optical microscopy*, pp. 121–224. Institute of Physics Publishing, New York.
8. Diaspro A. 1999. Introduction to two-photon microscopy. *Microsc Res Technol* **47**:163–164.
9. Lakowicz JR, ed. 1997. *Topics in fluorescence spectroscopy*, Vol. 5: *Nonlinear and two-photon-induced fluorescence*, Plenum Press, New York.
10. So PTC, Dong CY, Masters BR, Berland KM. 2000. Two-photon excitation fluorescence microscopy. *Annu Rev Biomed Eng* **2**:399–429.
11. Williams RM, Piston DW, Webb WW. 1994. Two-photon molecular excitation provides intrinsic 3-dimensional resolution for laser-based microscopy and microphotochemistry. *FASEB J* **8**:804–813.
12. Denk W, Piston DW, Webb WW. 1995. Two-photon molecular excitation in laser-scanning microscopy. In *Handbook of biological confocal microscopy*, pp. 445–448. Ed JB Pawley. Plenum Press, New York.

13. Goppert-Mayer M. 1931. Uber elementarakte mit zwei quantensprungen. *Ann Phys Leipzig* **9**:273–294.
14. Masters BR, So PTC. 2004. Antecedents of two-photon excitation laser scanning microscopy. *Microsc Res Technol* **63**:3–11.
15. Xu C, Webb WW. 1997. Multiphoton excitation of molecular fluorophores and nonlinear laser microscopy. In *Topics in fluorescence spectroscopy*, Vol. 5: *Nonlinear and two-photon-induced fluorescence*, pp. 471–540. Ed JR Lakowicz. Plenum Press, New York.
16. Xu C, Williams RM, Zipfel W, Webb WW. 1996. Multiphoton excitation cross-sections of molecular fluorophores. *Bioimaging* **4**: 198–207.
17. Xu C, Zipfel W, Shear JB, Williams RM, Webb WW. 1996. Multiphoton fluorescence excitation: new spectral windows for biological nonlinear microscopy. *Proc Natl Acad Sci USA* **93**:10763–10768.
18. Xu C, Webb WW. 1996. Measurement of two-photon excitation cross sections of molecular fluorophores with data from 690 to 1050 nm. *J Opt Soc Am B* **13**(3):481–490.
19. Xu C, Guild J, Webb WW. 1995. Determination of absolute two-photon excitation cross-sections by *in situ* second-order autocorrelation. *Opt Lett* **20**:2372–2374.
20. Kennedy SM, Lytle FE. 1986. P-bis(o-methylstyryl)benzene as a power-squared sensor for two-photon absorption measurements between 537 and 694 nm. *Anal Chem* **58**:2643–2647.
21. Courtesy of Drs. Zygmunt Gryczynski and Ignacy Gryczynski.
22. Birch DJS. 2001. Multiphoton excited fluorescence spectroscopy of biomolecular systems. *Spectrochim Acta, Part A* **57**:2313–2336.
23. Gryczynski I, Malak H, Lakowicz JR. 1996. Multiphoton excitation of the DNA stains DAPI and Hoechst. *Bioimaging* **4**:138–148.
24. Lakowicz JR, Gryczynski I, Malak H, Schrader M, Engelhardt P, Kano H, Hell SW. 1997. Time-resolved fluorescence spectroscopy and imaging of DNA labeled with DAPI and Hoechst 33342 using three-photon excitation. *Biophys J* **72**:567–578.
25. Lakowicz JR, Gryczynski I. 1992. Fluorescence intensity and anisotropy decay of the 4',6-diamidino-2-phenylindole–DNA complex resulting from one-photon and two-photon excitation. *J Fluoresc* **2**(2):117–122.
26. Callis PR. 1997. The theory of two-photon induced fluorescence anisotropy. In *Topics in fluorescence spectroscopy*, Vol. 5: *Nonlinear and two-photon induced fluorescence*, pp. 1–42. Ed JR Lakowicz. Plenum Press, New York.
27. Johnson CK, Wan C. 1997. Anisotropy decays induced by two-photon excitation. In *Topics in fluorescence spectroscopy*, Vol. 5: *Nonlinear and two-photon induced fluorescence*, pp. 43–85. Ed JR Lakowicz. Plenum Press, New York.
28. Callis PR. 1997. Two-photon induced fluorescence. *Annu Rev Phys Chem* **48**:271–297.
29. Lakowicz JR, Gryczynski I, Gryczynski Z, Danielson E, Wirth MJ. 1992. Time-resolved fluorescence intensity and anisotropy decays of 2,5-diphenyloxazole by two-photon excitation and frequency-domain fluorometry. *J Phys Chem* **96**:3000–3006.
30. Wan C, Johnson CK. 1994. Time-resolved two-photon induced anisotropy decay: the rotational diffusion regime. *J Chem Phys* **101**: 10283–10291.
31. Chen SY, Van Der Meer BW. 1993. Theory of two-photon induced fluorescence anisotropy decay in membranes. *Biophys J* **64**:1567–1575.
32. Gryczynski I, Malak H, Lakowicz JR. 1995. Three-photon induced fluorescence of 2,5-diphenyloxazole with a femtosecond Ti:Sapphire laser. *Chem Phys Lett* **245**:30–35.
33. Monson PR, McClain WM. 1970. Polarization dependence of the two-photon absorption of tumbling molecules with application to liquid 1-chloronaphthalene and benzene. *J Chem Phys* **53**(1):29–37.
34. Aleksandrov AP, Bredikhin VI, Genkin VN. 1971. Two-photon absorption by centrally symmetric organic molecules. *Soviet Phys JETP* **33**(6):1078–1082.
35. Mohler CE, Wirth MJ. 1988. Solvent perturbations on the excited state symmetry of randomly oriented molecules by two-photon absorption. *J Chem Phys* **88**(12):7369–7375.
36. Lakowicz JR, Gryczynski I, Kusba J, Danielsen E. 1992. Two photon-induced fluorescence intensity and anisotropy decays of diphenylhexatriene in solvents and lipid bilayers. *J Fluoresc* **2**(4): 247–258.
37. Lakowicz JR, Gryczynski I. 1997. Multiphoton excitation of biochemical fluorophores. In *Topics in fluorescence spectroscopy*, Vol. 5: *Nonlinear and two-photon induced fluorescence*, pp. 84–144. Ed JR Lakowicz. Plenum Press, New York.
38. Malak H, Gryczynski I, Dattelbaum JD, Lakowicz JR. 1997. Three-photon-induced fluorescence of diphenylhexatriene in solvents and lipid bilayers. *J Fluoresc* **7**(2):99–106.
39. Squirrell JM, Wokosin DL, White JG, Bavister BD. 1999. Long-term two-photon fluorescence imaging of mammalian embryos without compromising viability. *Nature Biotechnol* **17**:763–767.
40. Lakowicz JR, Gryczynski I. 1992. Tryptophan fluorescence intensity and anisotropy decays of human serum albumin resulting from one-photon and two-photon excitation. *Biophys Chem* **45**:1–6.
41. Kierdaszuk B, Gryczynski I, Modrak-Wojcik A, Bzowska A, Shugar D, Lakowicz JR. 1995. Fluorescence of tyrosine and tryptophan in proteins using one- and two-photon excitation. *Photochem Photobiol* **61**(4):319–324.
42. Lakowicz JR, Kierdaszuk B, Gryczynski I, Malak H. 1996. Fluorescence of horse liver alcohol dehydrogenase using one- and two-photon excitation. *J Fluoresc* **6**(1):51–59.
43. Lakowicz JR, Gryczynski I, Danielsen E, Frisoli J. 1992. Anisotropy spectra of indole and n-acetyl-L-tryptophanamide observed for two-photon excitation of fluorescence. *Chem Phys Lett* **194**(4,5,6):282–287.
44. Cramb DT, Wallace SC. 1998. The adsorption of L-tryptophan to the H_20–CCL_4 interface, monitored by red-edge two photon-induced polarized fluorescence. *J Fluoresc* **8**(3):243–252.
45. Lippitz M, Erker W, Decker H, van Holde KE, Basche T. 2002. Two-photon excitation microscopy of tryptophan-containing proteins. *Proc Natl Acad Sci USA* **99**(5):2772–2777.
46. Gryczynski I, Malak H, Lakowicz JR. 1996. Three-photon excitation of a tryptophan derivative using an fs-Ti:Sapphire laser. *Biospectroscopy* **2**:9–15.
47. Gryczynski I, Malak H, Lakowicz JR, Cheung HC, Robinson J, Umeda PK. 1996. Fluorescence spectral properties of troponin c mutant F22W with one-, two-, and three-photon excitation. *Biophys J* **71**:3448–3453.
48. Callis P. 1993. On the theory of two-photon induced fluorescence anisotropy with application to indoles. *J Chem Phys* **99**(1):27–37.
49. Rehms AA, Callis PR. 1993. Two-photon fluorescence excitation spectra of aromatic amino acids. *Chem Phys Lett* **208**(3,4):276–282.

50. Maiti S, Shear JB, Williams RM, Zipfel WR, Webb WW. 1997. Measuring serotonin distribution in live cells with three-photon excitation. *Science* **275**:530–532.
51. Gostkowski ML, Allen R, Plenert ML, Okerberg E, Gordon MJ, Shear JB. 2004. Multiphoton-excited serotonin photochemistry. *Biophys J* **86**:3223–3229.
52. Konig K. 2000. Multiphoton microscopy in life sciences. *J Microsc* **200**(2):83–104.
53. Blatter LA, Niggli E. 1998. Confocal near-membrane detection of calcium in cardiac myocytes. *Cell Calcium* **23**(5):269–279.
54. Niggli E, Egger M. 2004. Applications of multi-photon microscopy in cell physiology. *Front Biosci* **9**:1598–1610.
55. Fan GY, Fujisaki H, Miyawaki A, Tsay RK, Tsien RY, Ellisman MH. 1999. Video-rate scanning two–photon excitation fluorescence microscopy and ratio imaging with cameleons. *Biophys J* **76**:2412–2420.
56. Miyawaki A, Llopis J, Heim R, McCaffery JM, Adams JA, Ikura M, Tsien RY. 1997. Fluorescent indicators for Ca^{2+} based on green fluorescent proteins and calmodulin. *Nature* **388**:882–887.
57. Huang S, Heikal AA, Webb WW. 2002. Two-photon fluorescence spectroscopy and microscopy of NAD(P)H and flavoprotein. *Biophys J* **82**:2811–2825.
58. Konig K, Riemann I. 2003. High-resolution multiphoton tomography of human skin with subcellular spatial resolution and picosecond time resolution. *J Biomed Opt* **8**(3):432–439.
59. Bewersdorf J, Hell SW. 1998. Picosecond pulsed two-photon imaging with repetition rates of 200 and 400 MHz. *J Microsc* **191**(1): 28–38.
60. Courtesy of Dr. Ignacy Gryczynski.

PROBLEMS

P18.1. *Anisotropies of a Styrene Derivative*: Figure 18.26 shows the steady-state anisotropies of 4-Dimethylamino-ω-diphenylphosphinyl-*trans*-styrene (DPPS) in n-butanol. The anisotropies are higher for two-photon excitation than for one-photon excitation. In both cases the anisotropies are independent of temperature. Explain both results. The difference in anisotropy has been explained in the text, but not the reason for a constant anisotropy at all temperatures.

P18.2. In Figure 18.17 the density of datapoints is less with Ti:sapphire excitation (855 nm) than with dye-laser (570 nm) or frequency-doubled dye-laser (285 nm) excitation. Suggest reasons why this is the case.

P18.3. Explain the direction of the intensity ratio change shown in Figure 18.21.

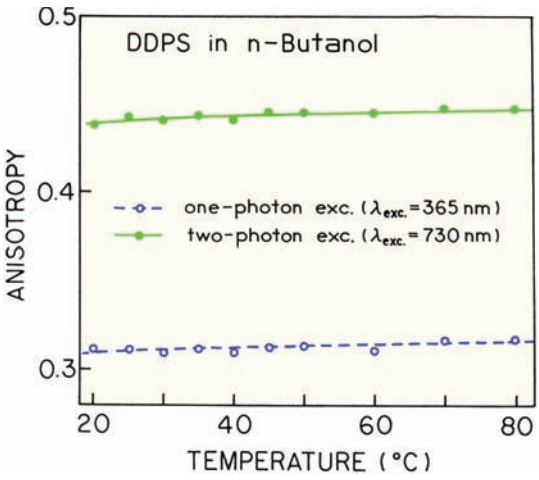

Figure 18.27. Steady-state anisotropies of DPPS. From [60].